JOURNAL OF PHYSICAL ORGANIC CHEMISTRY
J. Phys. Org. Chem. **12**, 837–842 (1999)

Reactions of 1,ω-bis(2-bromopyridinium)alkanes with azide ions: charge effect and intermediates

Maria da Graças Neves Corrêa,[1] Mario José Politi[2] and Noboru Hioka[1]*

[1]Departamento de Química, Universidade Estadual de Maringá, Maringá, Pr, Brazil
[2]Departamento de Bioquímica, Instituto de Química da Universidade de São Paulo, São Paulo, SP, Brazil

Received 4 August 1998; revised 2 December 1998; accepted 11 December 1998

ABSTRACT: The reaction between 1,ω-bis(2-bromopyridinium)alkanes (with 3, 4, 5, 6 and 8 methylene groups) with azide ions was examined to investigate the effects of charge proximity between the aromatic rings upon reactivity. ^{1}H and ^{13}C NMR spectra show the formation of a half-reacted intermediate having bromopyridinium and azidepyridinium extremities. Activation parameters for the reaction, ionic strength and solvent effects were investigated. An increase in reactivity was found with decrease in the methylenic chain length for both reactant and intermediate. The results are rationalized by the favorable formation of sandwich-type complexes between the pyridinium rings and the azide for the compounds with shorter methylenic spacers. Copyright © 1999 John Wiley & Sons, Ltd.

KEYWORDS: 1,ω-bis(2-bromopyridinium)alkanes; azide ions; charge effect; intermediates; sandwich complexes

INTRODUCTION

N-Alkyl-4-cyanopyridinium ions (RPCN) undergo alkaline hydrolysis to produce the corresponding *N*-alkyl-4-pyridone (P) and *N*-alkyl-4-carbamidopyridinium (A).[1] Both reaction rate constants and product composition (P/A) are dependent upon the medium, with the uncharged product (P) being favored in lower polarity media. The pH profile in aqueous solutions demonstrates that composition ratios (P/A) and reaction rate constants increase with increasing [OH^-].[2] For homologous RPCN compounds with R varying from methyl to dodecyl, reaction rate constants (excess of OH^-) are independent of [RPCN] up to 1×10^{-3} mol l^{-1} substrate. However, the hydrolysis reaction of the *N*-hexadecyl/derivative (HCP), a surfactant monomer, showed increased rate constants and P/A ratios with [HCP] concentrations up to three orders of magnitude lower than its critical micelle concentration.[3] These data were interpreted in terms of increased reactivity and preference for OH^- attack at the 4-position of the pyridinium ring of HCP small premicellar aggregates such as dimers and trimers whose existence was shown by kinetic, conductivity and fluorimetric determinations.[3–5]

To model the increased reactivity of a pre-micellar aggregate, the alkaline hydrolysis reaction of a series of homologous bis-positive dimers containing two reactive groups linked by methylene spacers of different lengths, 1,ω-bis(2-bromopyridinium)alkanes (RPBr) [with R propane (**I**), butane (**II**), pentane (**III**), hexane (**IV**) and octane (**V**)] were investigated.[6] The reaction kinetics of **I**–**V** (OH^- excess) fitted a two consecutive first-order process, corresponding to a fast initial attack leading to the half-reacted product, the 1-(2-pyridone)-3-(bromopyridinium)alkane bromide, followed by the *ca* eightfold slower formation of the respective uncharged bis(2-pyridone). On the basis of the reactivity order of the first step (**I** > **II** > **III** > **IV** > **V**) and the invariant nature of the slow step, a through-space charge effect was postulated, originating from the stability of the initial charge-transfer complex between the nucleophile and the bis-charged reactant.

In order to investigate further the charge effect, it was of interest to study a simpler reaction, which experienced no net charge change. Thus, the reaction of *N*-methyl-2-bromopyridinium (MBrP) with sodium azide (NaN_3) produced the corresponding *N*-methyl-2-azidepyridinium bromide by nucleophile substitution at C-2.[7] The present work, involving kinetic studies of the reaction of N_3^- with RPBr (**I**–**V**), was undertaken in order to compare the effects of the spacer length between the pyridinium rings on reaction rates.

EXPERIMENTAL

1,ω-Bis(2-bromopyridinium)alkanes, bromide salts (RPBr) [R = propane (**I**), butane (**II**), pentane (**III**),

**Correspondence to:* N. Hioka, Departamento de Química, Universidade Estadual de Maringá, Av. Colombo, 5790 Maringá, Paraná (Pr), Brazil.
E-mail: petdqi@uem.br
Contract/grant sponsor: CNPq.
Contract/grant sponsor: CAPES.

CCC 0894–3230/99/110837–06 $17.50

hexane (**IV**) and octane (**V**)] were synthesized as described previously[6] and characterized by UV–VIS, ^{1}H NMR and ^{13}C NMR (normal and DPT-135) spectroscopy. The final products of the reaction of RPBr with excess N_3^- (reaction in D_2O) were characterized by UV–VIS, ^{1}H NMR and ^{13}C NMR (normal, DPT-135 and HETCOR) spectroscopy. Reaction intermediates were obtained by conducting the reaction under stoichiometric conditions of RPBr (0.058 mmol) with N_3^- (0.058 mmol) in 0.6 ml of D_2O. Unfortunately, the reaction mixtures were contaminated with unreacted reagent and final product and further purification was not possible. However, ^{1}H and ^{13}C NMR spectra for the intermediates **I**, **II** and **III** were obtained and properly assigned (Table 1).

Kinetic assays were conducted under pseudo-first-order conditions (excess of N_3^-) and were recorded using a Beckman DU-70 UV–VIS spectrophotometer following either consumption of the reactants (277 nm) or the appearance of products (294 nm). All runs were performed at 30.0 °C, except for the activation parameter measurements, which were obtained by determining observed rate constants (k_{obs}) from 10.0 to 60.0 °C. Aqueous stock solutions of NaN_3 and RPBr were prepared with deionized, distilled and boiled under nitrogen-purged water. Stock solutions were stored in the dark. The k_{obs} values were calculated using a single exponential equation. The order of the reactions was determined using [NaN_3] in the range 0.10–1.00 mol l^{-1} and the ionic strength (μ = 1.00 mol l^{-1}) was maintained with KCl. Specific salt effects were investigated with KCl, KBr and Kl. For the study of the ionic strength effect, KCl concentrations were varied between 0.00 to 1.30 mol l^{-1} and NaN_3 concentrations were fixed at 0.75 mol l^{-1}. Dielectric constant effects were investigated using varying amounts of 1,4-dioxane in water.

RESULTS AND DISCUSSION

The aim of this work was to investigate the effect of charge proximity on the reactivity of substrates with two equivalent reaction centers. For this purpose the reaction depicted in Scheme 1 was selected where the transformation of the RPBrs into the half-reacted product (intermediate) and final product occurs in two consecutive steps. Evidence for the validity of this mechanistic proposal will be presented below.

Table 1 summarizes the NMR data for the compounds depicted in Scheme 1. In this table and in the following discussion, data are arranged according to the compound name (number) that is the starting material (denoted Reag), final material (denoted Prod) or reaction intermediate species (denoted Mixt-Reag and Mixt-Prod).

The proton NMR spectra for the RPBrs (Reag) are similar (Table 1). In Scheme 1, hydrogen and carbon atoms are numbered in order to identify their assignments. The peak attribution starting from low field is as follows: (i) the H-6 chemical shift appears as a doublet at ~9.1; (ii) H-4 and H-3 (superimposed) appear as doublets at ~8.4; (iii) H-5 appears as a multiplet at ~8.1; (iv) H-7 and other methylenic protons where the first to appear is that from the vicinal C—H group to the N atom appear below ~5.0. These attributions are based on the following arguments: (i) H-6 suffers a strong deshielding effect by the vicinal N^+ center; (ii) H-4 is also affected by the N^+ group since in the resonant structures the positive charge can be located at C-4; (iii) H-3 and H-5 are influenced by the '+*M*' effect of the bromine group where, for the case of H-3, the '−*I*' effect of the bromine atom acts in an opposite direction and therefore the H-5 signal is more shielded than that of H-3; and (iv) in the methylenic chain the order of chemical shifts corresponds to the distance from the N^+ atom, thus H-7 is more deshielded and the remaining protons signals appear subsequently. These assignments are in agreement with these reported for 1*H*-pyridinium[8] and for *N*-methyl-2-bromopyridinium.[9]

The assignment of the RPBr ^{13}C NMR spectra follows the order found for the ^{1}H NMR spectra. Thus C-6 and C-4 are the more deshielded peaks (Table 1). Subsequently the signal at ~141 *ppm* appears due to C-2 which is affected by the vicinal bromine group [DPT-135 NMR (not shown) suppresses this peak, confirming this attribution]. C-3 and C-5 are the next signals and finally the methylenic carbons appear in the same order as for the corresponding ^{1}H signals.

The NMR data for the final products, Prod (Table 1), also show similar peaks for the derivatives studied and follow the same trend as above. The H-6 proton is the most deshielded due to its proximity to the N^+ atom. Then the H-4 peak appears since the azide group exerts a mesomeric donor effect which in turn shields H-3 and H-5 atoms, yielding smaller chemical shifts. Next the methylenic protons signals are seen. These signals match the attributions by Bunton and Cvenca[7] for *N*-methyl-2-azidepyridinium bromide. The ^{13}C NMR data for the final product show that azide substitution leads to a deshielding effect of ~13 ppm on C-2 and shielding of ~16 ppm on C-3 and of ~5 ppm on C-5, C-6 and C-7 atoms, with little effect on the remaining carbons. For C-2 the attribution was confirmed by DPT-135 analysis (not shown). The correlations between protons and carbons were confirmed by HETCOR and COSY spectra (not presented). Furthermore, spectral integration for reagents and final products agreed with the assignments made.

In the case of the intermediate reaction species, we were unable to purify them once they were contaminated with initial and final product materials (as mentioned in the Experimental section). For clarity, NMR data for the intermediates in Table 1 were purposely arranged as 'Mixt-Reag' and 'Mixt-Prod' in order to show their relationship with the signals of pure reagent or pure product, i.e. for a given RPBr, Mixt-Reag and Mixt-Prod belong to the same spectrum; data are presented in

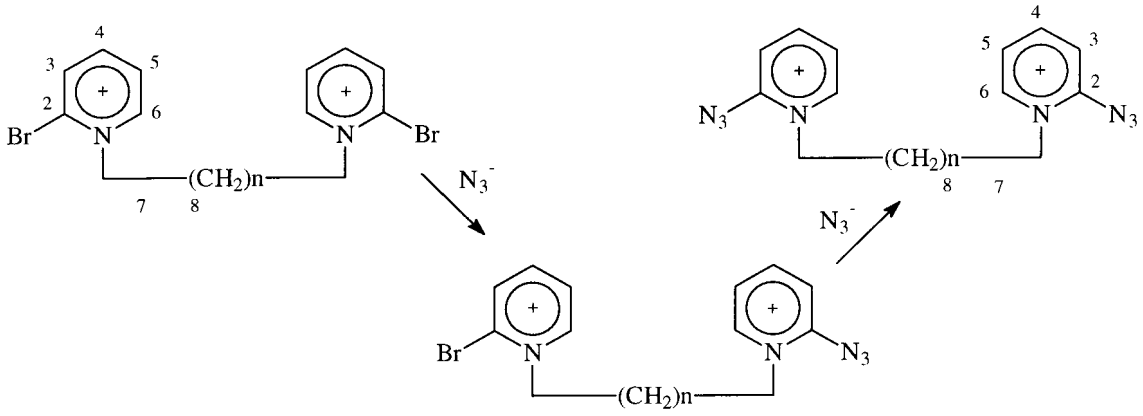

Scheme 1

Table 1. ^{1}H NMR and ^{13}C NMR data (δ, ppm) for substrates **I, II, III** and **V**, the corresponding final products and intermediate reaction mixtures[a]

Compound	C-2	H-3 C-3	H-4 C-4	H-5 C-5	H-6 C-6	H-7 C-7	H-8 C-8	H-9 C-9	H-10 C-10
I Reag		8.44,d	8.44,d	8.11,m	9.13,d	5.07,t	2.80,m		
	141.79	138.12	150.13	130.61	150.76	62.03	31.87		
I Prod		7.99,d	8.55,t	7.73,t	8.67,d	4.69	2.63,q		
	155.00	122.23	150.16	125.60	146.94	56.27	31.45		
I Mixt		8.44	8.44	8.12	9.14	5.05	2.80		
Reag	141.75	138.15	150.11	130.64	150.79	62.44	31.90		
	141.64	138.12	150.07	130.59	150.75	62.06	31.60		
I Mixt		8.00	8.52	7.73	8.69	4.72	2.70		
Prod	154.98	122.26	150.22	125.57	146.92	56.17	31.35		
	154.72	122.22	150.17	125.51	146.88	55.82			
II Reag		8.42,d	8.42,d	8.08,m	9.04,d	4.94,t	2.24,m		
	141.34	137.94	149.63	130.29	150.48	64.96	28.64		
II Prod		7.95,d	8.48,t	7.68,t	8.58,d	4.56,m	2.07,m		
	154.77	121.96	149.67	125.28	146.79	58.84	28.55		
II Mixt		8.41	8.41	8.08	9.03	4.91	2.24		
Reag							2.16		
	141.34	137.91	149.57	130.21	150.46	65.06	28.81		
						64.96	28.29		
II Mixt		7.97	8.48	7.68	8.60	4.58	2.07		
Prod	154.70	121.96	149.64	125.22	146.73	58.69	28.44		
						58.60	28.29		
III		8.38,d	8.38,d	8.06,m	9.01,d	4.83,t	2.12,q	1.63,q	
Reag	141.32	137.91	149.46	130.26	150.51	65.68	31.54	25.07	
III Prod		7.94,d	8.48,t	7.68,t	8.58,d	4.51,t	2.03,q	1.50,q	
	154.57	121.84	149.40	125.12	146.73	59.31	31.10	25.21	
III Mixt		8.40	8.40	8.07	9.03	4.85	2.13	1.58	
Reag	141.26	137.83	149.46	130.18	150.43	65.65	31.49	25.04	
								25.12	
III Mixt		7.96	8.48	7.68	8.60	4.52	2.05		
Prod	154.62	121.94	149.37	125.15	146.77	59.28	31.10	25.21	
V Reag		8.38,d	8.38,d	8.06,t	9.02,d	4.80	2.03,q	1.43,s	1.43,s
	141.16	137.76	149.17	130.06	150.40	66.19	31.93	30.75	28.00
V Prod		7.93,d	8.48,t	7.68,t	8.58,d	4.49,t	1.95,m	1.40,s	1.40,s
	154.53	121.87	149.28	125.12	146.80	59.87	31.64	30.84	28.20
V Mixt		8.40	8.40	8.07	9.04	4.82	2.05	1.46	1.46
Reag	141.11	137.68	149.09	130.00	150.34	66.12	31.86	30.67	27.94
V Mixt		7.96	8.48	7.68	8.60	4.49	1.96	1.41	1.41
Prod	154.42	121.82	149.19	124.98	146.71	59.70	31.51	30.72	28.06

[a] Solvent, D_2O; reference, TMS.

different rows only to emphasize their similarity with non-reacted or fully reacted pyridinium moieties. For example, C-2 data for **I** show a reagent peak at 141.79 ppm and a product peak at 155.00 ppm, whereas in the spectrum for the mixture four peaks were observed at 141.75, 141.64, 154.98 and 154.72 ppm (Table 1). These transitions correspond to the reagent and intermediate having a similarity with the reagent (peaks at 141.75 and 141.64 ppm) and the product and part of the intermediate similar to the product (peaks at 154.98 and 154.72 ppm). Although it is tempting to correlate the closest band to that of the pure species, such assignment would be incorrect since there is no exact theory capable of predicting where the split signal should appear. Moreover, since the amount of reagent and product contamination in the mixture (intermediate) at this stage are unknown it would be worthless to conduct further analysis on these data. However, ^{1}H NMR and ^{13}C NMR spectra of the mixture exhibit split signals matching those of the reactant (two 2-bromopyridinium heads) and of the final product (two 2-azidepyridinium moieties).

For the reaction of **III**, ^{1}H NMR signals from the central protons (H-9) of the reagent and final product appeared at 1.63 and 1.50 ppm, respectively; for the mixture, a multiplet is observed at 1.58 ppm (Table 1). These peaks could be simply a coalescence of the reactant and final product signals. However, in the ^{13}C spectrum of the mixture the signal due to C-9 presents an additional peak at 25.12 ppm, besides those of the reactant (25.04 ppm) and product (25.21 ppm) (Table 1). This signal is assigned to the intermediate. It should be noted that for bridged compounds the loss of symmetry in the molecule leads to the appearance of one peak for the central C atom for linkers with an odd number of atoms and two peaks for linkers having an even number of carbons (two central carbons).[10,11] Thus, in a mixture having reactant, final product and intermediate, the spectra for these central carbons will contain three peaks for odd linkers and four peaks for even linkers. This effect will be more evident in compounds having shorter spacers since the rotational stress will be larger.

For compound **II** the H-6 doublet peak at 9.04 ppm shows a well resolved additional duplication in the mixture. The other peaks of the reagent and product are broadened with less evident duplication. In effect, assignment of the complex spectrum of the mixture was difficult to rationalize. However, the H-8 band in the mixture shows, besides the reagent peak at 2.24 ppm and that due to the product at 2.07 ppm, a multiplet signal at 2.16 ppm attributed to the intermediate. The carbon spectrum of the mixture once again shows reagent and product signals but C-7 and C-8 peaks are duplicated with a 0.1 and 0.2 ppm difference, respectively (Table 1). In comparison, for the single central carbon in the mixture from **III**, the spectrum showed a triplicate peak deriving from the reagent, product and intermediate.

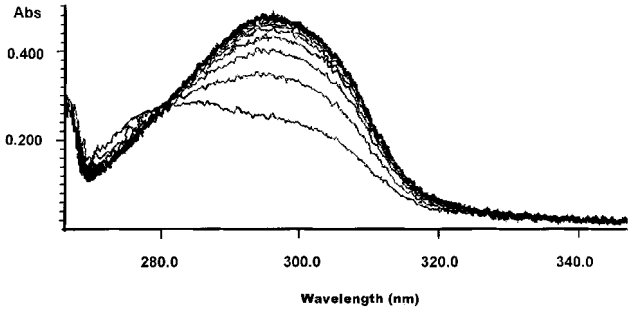

Figure 1. Successive UV–VIS spectra for reaction of compound **I** with azide ions. $[N_3^-] = 1.00$ mol l^{-}, [**I**] = 2.2×10^{-5} mol l^{-1}, $T = 30.0$ °C, time range = 20 s. Note the isosbestic point at 281 nm

Following the same pattern, for **I** the doublet transitions at 9.13 (H-6) and 8.44 ppm (H-3 and H-4) are duplicated in the mixture. Again, the product doublet peaks at 8.67 (H-6) and 7.99 ppm (H-3) appear duplicated in the spectrum of the mixture. The peaks of the aromatic carbons of the mixture from **I** are duplicated compared with the reagent or product. Shifts in the signal position were generally small (~0.05 ppm) with the exception of C-2, where shifts of 0.11 and 0.26 ppm relative to the reagent and final product, respectively, were observed (Table 1). The signals of the aliphatic carbon C-7 for reagent and product were duplicated in the mixture (0.4 ppm difference), whereas for the central carbon C-8, which as for the mixture derived from **III**, were triplicated (0.3 ppm difference). This duplication of signals and the extra peak in the case of C-8 again strongly suggest the presence of the intermediate species in the mixture.

The ^{1}H and ^{13}C NMR spectra of the mixture for the reaction of **V** with azide exhibited peaks identical with the reagent and final product, not allowing characterization of the intermediate species. This can be rationalized by considering the long distance between the aromatic rings, which diminishes any effects from symmetry break in the intermediate due to the conformational freedom.

Having qualitatively established the occurrence of an intermediate species resembling a half reactant–half product compound, the next objective is to unravel the kinetic nature of the reaction. N_3^- substitution on RPBrs can be readily monitored by following either the reactant consumption by the absorbance decrease at 277 nm or the product formation, seen as an increase in absorption at 294 nm. This behavior is shown in Fig. 1 for the reaction of **I** with N_3^-, where a single isosbestic point at 281 nm can be observed. For compound **V** the time dependence of the absorbance change at 294 nm (or 277 nm) fitted to a simple first-order process with a correlation coefficient (*r)* of 0.99999. Interestingly, the presence of an isosbestic point and the fit to a first-order equation usually indicate only two species (no intermediates formed during the reaction). However, for the shorter RPBrs the quality of fit (based on *r* values) diminishes, suggesting a slight

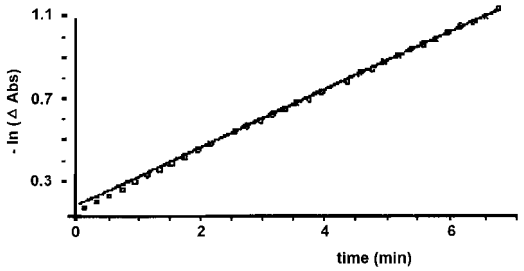

Figure 2. Mathematical treatment of the first-order equation for the reaction of **I** with azide ions. Absorbance at 294 nm. $[N_3^-] = 1.00$ mol l^{-1}, $[\mathbf{I}] = 2.2 \times 10^{-5}$ mol l^{-1}, $T = 30.0$ °C. $r = 0.998$. Line, theoretical curve; □, experimental points

deviation of the exponential law, as for compound **I** where $r = 0.998$ (Fig. 2). These deviations suggest the presence of two kinetically distinguishable reaction steps, i.e. intermediate formation, in accordance with NMR results. Considering, however, that there is no net charge variation in the reaction, the second step should present about the same reactivity as the initial one. Thus the two consecutive reaction steps should not be differentiated as in the case of the alkaline reaction,[6] where the monopositive intermediate has about an eightfold decreased reactivity because of its lower charge.

The overall observed rate constants (k_{obs}) for azide substitution on RPBrs are collected in Table 2. Clearly, at a given azide concentration and fixed ionic strength, the reaction order is **I** > **II** > **III** > **IV** > **V**. For **I**, k_{obs} is about double that for **II**, which in turn is about 2–3-fold faster than those for the remaining compounds. Slopes of log k_{obs} *versus* log $[N_3^-]$ plots (not shown) were 0.94 ± 0.03, indicating the same type of reaction for the RPBrs investigated. Increased reactivities for the compounds having shorter methylene spacers are in agreement with that found in pre-micellar aggregates[3] or in RPBr alkaline hydrolysis.[6]

The effect of ionic strength (μ) on the reaction of **I** and **V** with azide is summarized in Table 3. The expected

Table 2. Observed rate constants (k_{obs}) for azide substitution on RPBr[a]

$[NaN_3]$ (mol l^{-1})	k_{obs} (min^{-1})				
	I	**II**	**III**	**IV**	**V**
1.00	1.413	0.523	0.258	0.203	0.153
0.90	1.383	0.434	0.253	0.176	0.135
0.80	1.361	0.429	0.226	0.165	0.126
0.70	1.089	0.407	0.207	0.146	0.108
0.60	0.843	0.305	0.163	0.129	0.093
0.50	0.816	0.287	0.140	0.105	0.079
0.40	0.590	0.216	0.109	0.084	0.067
0.30	0.478	0.166	0.099	0.073	0.053
0.20	0.386	0.119	0.065	0.047	0.036
0.10	0.160	0.062	0.033	0.026	0.020

[a] $[NaN_3] = 0.10$ –1.00 mol l^{-1}, $\mu = 1.00$ mol l^{-1} (KCl addition), $T = 30.0$ °C.

Table 3. Effect of ionic strength (μ) on k_{obs} for compounds **I** and **V** with variable [KCl][a]

[KCl] (mol l^{-1})	μ	k_{obs} (min^{-1})	
		I	**V**
0.00	0.75	1.229	0.127
0.10	0.85	1.289	0.138
0.25	1.00	1.139	0.136
0.30	1.05	0.920	0.096
0.50	1.25	0.914	0.086
0.70	1.45	0.895	0.100
0.90	1.65	0.843	0.096
1.10	1.85	0.821	0.095
1.30	2.05	0.770	0.091

[a] $[NaN_3] = 0.75$ mol l^{-1}, $T = 30.0$ °C.

decrease in k_{obs} with increase in μ for a reaction between oppositely charged reactants is observed. The effect is slightly more pronounced for **I**, where the charge density is higher.

The specific salt effects are presented in Table 4 for the reactions of **I** and **V**. The inhibitory effect is KCl < KBr <Kl, following the usual liotropic series.[12] The larger inhibitory effect observed for iodide is assigned to the higher polarizability, implying the presence of stronger short-range interactions with the pyridinium rings. This effect correlates with the charge transfer complex formation between pyridinium and iodide ions.[13]

From the temperature dependence on the reaction of azide ion with compounds **I** and **V**, straight Arrhenius plots were obtained (not shown) and the calculated activation parameters are presented in Table 5. For comparison, values obtained for the alkaline hydrolysis of compound **I**,[6] of *N*-methyl-2-bromopyridinium (MBrP),[9] of *N*-methyl-4-cyanopyridinium (MPC)[14] and of 1,3-bis(4-cyanopyridinium)propane (CPP)[14] are included. The hydrolysis reaction of MBrP and MPC (monocharged) occurs in one step whereas for the other two the reaction (bis-positive reagent) occurs in a fast initial step followed by slow decomposition of the intermediate (monocharged species) into the final products. It can be observed that the reactions involving doubly charged species present $\Delta S^{\circ\neq}$ around −12 to −14 cal mol^{-1} K^{-1} whereas for the monocharged species the

Table 4. k_{obs} obtained for compounds **I** and **V** in NaN_3 (0.75 mol l^{-1}) and halides at 30.0 °C

Salt	Concentration (mol l^{-1})	k_{obs} (min^{-1})	
		I	**V**
KCl	0.25	1.139	0.137
	1,00	0.788	0.098
KBr	0.25	0.962	0.113
	1,00	0.692	0.086
Kl	0.25	0.973	0.103
	1,00	0.618	0.070

Table 5. Activation energy ($E_a^{\circ\neq}$) and entropy ($\Delta S^{\circ\neq}$) for reaction of **I** and **V** with N_3^- and of MBrP, **I**, **V**, MPC and CPP with OH^-

Reaction	$E_a^{\circ\neq}$ kcal mol^{-1})	$\Delta S^{\circ\neq}$ (cal mol^{-1} K^{-1})
MBrP–OH^-[a]	15.75	−8.33
I–OH^-[b] (fast)	12.47	−13.38
I–OH^-[b] (slow)	15.37	−8.14
MPC–OH^-[c]	14.89	−9.63
CPP–OH^-[c] (fast)	12.52	−12.14
CPP–OH^-[c] (slow)	14.48	−8.96
I–N_3^-	16.99	−14.05
V–N_3^-	18.63	−13.42

[a] Data from Ref. 9.
[b] Data from Ref. 6.
[c] Data from Ref. 14.

$\Delta S^{\circ\neq}$ values are around −8 to −10 cal mol^{-1} K^{-1} (1 cal = 4.184 J). Furthermore, these values contrast with the positive $\Delta S^{\circ\neq}$ values found for a pure electrostatic driven process.[15] This unfavorable activation entropy for the doubly charged compounds is compensated by the activation energy of the process when compared with the monocharged (difference of 2–3 kcal mol^{-1}).

In order to investigate solvent effects on the reaction, dioxane–water mixtures were employed (Table 6). As expected, reaction rate enhancement is observed for a reaction between oppositely charged ions with decrease in the dielectric constant of the medium. Interestingly, the increase in the rate constants on going from pure water to 35% dioxane are ∼40-fold for **V** and ∼15-fold for **I**. Again, this result suggests that the reactivities are not determined by a simple electrostatic effect. Applying the Brønsted–Bjerrum model[15–17] for these sets of data resulted in a reasonably linear dependence of lnk *versus* $1/\epsilon$ plots which showed positive slopes appropriate for a reaction between opposite charges.[18] The slope found for the reaction of **I** is 312 and that for **V** is 402. From these slopes the distance of closest (dc) approach in the activated complex was estimated. For **I** dc = 3.5 Å and for **V** dc = 2.7 Å, in accordance with closest packing for **V** and the azide ion.

The difference in dc values can be interpreted by the formation of distinct ion pairs. In the case of **V** the pair would involve a single pyridinium ring, whereas for **I** the pair would include both rings in a type of sandwich complex. Another possibility is the ease of chain rotation for the longer spacer to accommodate the azide ion between the two pyridinium rings. The difference found in the activation energies for the reaction of **I** and of **V** also shows higher reactivity for **I** (Table 5). Once nucleophillic attack is the rate-controlling step for the azide–bromopyridinium reaction for either the intermediate or final product formation, the observed differences in reactivities must derive from a distinct conformation of the intimate pair or in the caging of the reactants. In other words, for shorter spacers the presence of the anion would be sensed by the two positive charges and favor a complex having the nucleophile intercalated between the cationic rings. For the longer spacers this effect would be less pronounced and the reaction thus occurs as having independent reaction centers.

Table 6. k_{obs} for **I** and **V** in water–dioxane solution[a]

Dioxane (%, v/v)	Dieletric constant[b]	k_{obs} (min^{-1})		$k_{\mathbf{I}}/k_{\mathbf{V}}$
		I	**V**	
0	76.72	0.305	0.029	10.5
10	67.79	0.652	0.076	8.6
20	58.90	1.426	0.202	7.1
30	50.11	3.336	0.499	6.7
35	45.78	4.845	1.160	4.2

[a] $[N_3] = 5.0 \times 10^{-2}$ mol l^{-1}, $T = 30.0$ °C
[b] from Ref. 2.

In conclusion, the reaction of bis-positive ions with azide ions, despite the presence of an isosbestic point and good adjustment to a linear first-order treatment, exhibited the formation of an intermediate as demonstrated by NMR analysis. Kinetic analysis showed the effect of the length of methylenic chain, favoring a sandwich type of complex for the shorter spacers and higher reactivities.

Acknowledgements

We express our gratitude to the Brazilian grant agencies CNPq and CAPES.

REFERENCES

1. E. M. Kosower and J. N. Patton, *Tetrahedron* **22**, 2081 (1966).
2. M. J. Politi and H. Chaimovich, *J. Phys. Org. Chem.* **4**, 207 (1991).
3. N. Hioka, M. J. Politi and H. Chaimovich, *Tetrahedron Lett.* **30**, 1051 (1989).
4. J. H. Fendler, *Membrane Mimetic Chemistry*. Wiley–Interscience, New York (1982).
5. C. A. Bunton and G. Savelli, *Adv. Phys. Org. Chem.* **22**, 213 (1986).
6. C. Fernandez, V. G. Toscano, H. Chaimovich, M. J. Politi and N. Hioka, *J. Phys. Org. Chem.* **11**, 25 (1998).
7. C. A. Bunton and A. Cuenca, *J. Org. Chem.* **52**, 901 (1987).
8. E. Pretsch, T. Clerc, J. Seibl and W. Simon, *Tablas para la Elucidacion Estrutural de Compuestos por Metodos Espectroscopicos*. Editorial Alhambra, Madrid (1980).
9. G. B. Barlin and J. A. Benbow, *J. Chem. Soc., Perkin Trans.* **2**, 790 (1987).
10. W. B. Jennings, *Chem. Rev.* **75**, 307 (1975).
11. K. Mislow and M. Raban, *Top. Stereochem*. **1**, 1 (1967).
12. L. R. Romsted, Ph D Thesis, Indiana University (1975).
13. E. M. Kosower, *An Introduction to Physical Organic Chemistry*. J Wiley, New York (1968).
14. N. Hioka, Ph D Thesis, University of São Paulo (1992).
15. K. J. Laidler, *Chemical Kinetics*, 3rd ed. Harper Collins, New York (1987).
16. J. H. Espenson, *Chemical Kinetics and Reactions Mechanism*. McGraw-Hill, New York (1981).
17. A. A. Frost and R. G. Pearson, *Kinetics and Mechanism*, 2nd ed. Wiley, New York (1961).
18. C. V. King and J. J. Josephs, *J. Am. Chem. Soc.* **66**, 767 (1944).